



White Shark Optimizer for Multi-Objective Optimal Allocation of Photovoltaic Distribution Generation in Electrical Distribution Networks Considering Different Kinds of Load Models and Penetration Levels

Anitha M^{1*} Kotaiah N.C¹ Rajesh Patil² Nagaraja Kumari CH³

¹R.V.R & J.C. College of Engineering, Chowdavaram, Guntur, Andhra Pradesh 522019, India

²SVERIS College of Engineering, Pamdharpur, Solarpur, Maharashtra, 413304, India

³Guru Nanak Institute of Technology, Ibrahimpatnam, Telangana 501506, India

* Corresponding author's Email: nrkumari84@gmail.com

Abstract: In recent times, reduction of greenhouse gas (GHG) emission in conventional power grids becomes most important towards global sustainability. Thus, adaption of renewable energy (RE) sources in electricity sector has become alternative solution. Photovoltaic (PV) technology has become most adapted RE technology even at small scale consumers levels due to their clean and noiseless operation, low investment and operational cost and easy to install and maintenance. In this paper, a new heuristic approach white shark optimizer (WSO) is introduced for solving the PV based distribution generation (DG) in electrical distribution networks (EDNs). Loss minimization, voltage profile improvement and reduction in GHG emission are considered for formulating the proposed multi-objective function. Simulation studies are performed on IEEE 33-bus EDN for different kinds of load penetrations. The computational efficiency of WSO is quantified using 50 independent simulations and compared with various other recent algorithms such as pathfinder algorithm (PFA), mayfly optimization algorithm (MOA), coyote optimization algorithm (COA), and future search algorithm (FSA). In various case studies, WSO has resulted for best solution than compared algorithms. A similar kind of overall improvement is observed even for increased load penetration levels along with improved voltage profiles by having PV based DGs in EDN optimally.

Keywords: Photovoltaic system, Electrical distribution system, Greenhouse gas emission, Loss reduction, Load models, Voltage stability enhancement, White shark optimizer.

1. Introduction

Electrical distribution networks (EDNs) are suffering as a result of low investment and a constant increase in demand for electricity. Furthermore, the vast majority of EDNs are constructed in radial arrangement with high X/R ratio branches, resulting in substantial losses and a low voltage profile. However, increasing global warming and greenhouse gas (GHG) emissions from conventional power plants have become a major cause of concern for those who want to upgrade traditional power systems to use clean and renewable energy (RE) sources instead of fossil fuels. Integration of RE as distribution generation (DG) in electric distribution networks (EDNs) has

received significant attention in recent years due to a variety of technological, economic, and environmental objectives. Among different RE technologies, photovoltaic (PV) and wind turbine (WT) based DGs have become popular. For either single or multiple objective functions like as loss minimization, voltage profile improvement, voltage stability enhancement, operating cost minimization, GHG emission reduction, and other factors have been proposed in the literature for optimal allocation of RE-based DGs. As a multi-variable optimization issue, the optimal allocation of DGs problem should be handled as a discrete-variable problem with the identification of locations as discrete variables and the evaluation of correct sizes as continuous variables. Aside from that, search variables are

constrained by lower and higher bounds as well as equal constraints. In order to address these issues, a variety of heuristic techniques have been developed by various academics.

In [1], salp swarm algorithm (SSA) is modified for the purpose of determining the optimal allocation of RE-based DGs in IEEE 33- and 69-bus RDSs while taking into account loss minimization, voltage profile improvement, voltage stability enhancement, operational cost minimization, and greenhouse gas (GHG) emission reduction. For increased performance and economic operation of RDNs, an enhanced grey wolf algorithm (EGWA) is used in [2] to determine the most optimal placements, sizes, and numbers of DGs, capacitor banks (CBs), and voltage regulators (VRs). Particle swarm optimization (PSO) is used in [3] to solve problems related to PV-based distributed generation (DG) systems, including as power and voltage quality difficulties, congestion, reactive power compensation, and safety concerns. As shown in [4], the optimal integration of active and reactive power-based DGs allocation in the IEEE 69-bus is solved by incorporating generic analytical expressions (GAE) into an optimal power flow model (OPF). When attempting to solve the problem, the primary focus is on loss minimization and voltage profile improvement. In [5], a fuzzy logic-based grasshopper optimization algorithm (GOA) is developed for solving optimal DGs, CBs, and EVs in the IEEE 69-bus with the goal of loss minimization and voltage profile improvement. It is proposed in [6] to use the water cycle algorithm (WCA) to address the DGs/CBs allocation problem for a variety of technological, economic, and environmental objectives. This problem is tackled in [7] by combining elements of the EGWA and the PSO to provide an optimal allocation of DGs/CBs that is based on techno-economic-environmental objectives. In [8], the differential evolution (DE) algorithm is used to integrate DGs with power factor controllers in order to provide active and reactive power compensation and, as a result, to achieve loss reduction and improvement in voltage profile. It is proposed in [9] to use the Archimedes optimization algorithm (AOA) to solve PV-based DGs in agricultural feeders with a view to achieving techno-environmental objectives. In [10], the improved harris hawks optimizer (IHHO) is used in conjunction with the PSO to solve stochastic PV and WT based DGs in RDNs with the goal of reducing loss and improving voltage profile, respectively. When solving the DGs allocation problem as a

single or multi-objective optimization problem using IHHO and MOIHHO, the authors treat loss minimization, voltage profile improvement, and voltage stability enhancement as primary objectives [11]. In [12], it is proposed to use an extended genetic algorithm (EGA) for the simultaneous allocation of DGs and CBs in RDNs while taking into account loss minimization, installation and operational cost optimization, and other factors. [13] shows how butterfly optimization algorithm (BOA) may be used to solve the problem of DGs allocation in RDNs while taking into account loss minimization and voltage profile enhancement. It is proposed in [14] to use a modified Jaya algorithm to deal with the PV-based DG allocation problem, with the goal being to maximize the PV penetration level while both reducing losses and improving the voltage profile. DG allocation problems with technological and economic objectives are addressed in [15] by a fuzzy-decision based multi-objective sine cosine algorithm (MOSCA) based on fuzzy decision making.

From the above discussed literature, optimal allocation of DGs in EDNs can result for multi-objective benefits. Due to multi-objectives, multi-type variables, and equal and unequal constraints, heuristic approaches have been adapted highly to solve these problems. In the current energy systems, researchers are increasingly focused on developing new algorithms that are faster and more efficient when solving such complicated and large-scale multi-objective optimization problems. The algorithms considered in the literature, on the other hand, have a number of shortcomings, such as slow convergence, being computationally expensive, and having difficulties maintaining the variety among the possible solutions. In recent times, mixed leader based optimizer (MLBO) [16], three influential members based optimizer (TIMBO) [17], darts game optimizer (DGO) [18], mixed best members based optimizer (MBMBO) [19], multi leader optimizer [20], random selected leader based optimizer [21], equilibrium optimizer (EO) [22], and white shark optimizer (WSO) [23], are some of such recent meta-heuristic algorithms. In these aspects, the following are the major contributions of this paper.

- 1) Solving the optimal allocation of PV-based DGs problem for multi-objectives includes loss minimization, voltage profile improvement and GHG reduction.
- 2) First application of white shark optimizer (WSO) for handling DG allocation in EDN.

- 3) Extension of DG allocation problem for different kinds of loads such as residential, industrial, commercial and their different penetration levels.
- 4) Comparison of WSO performance with other recent algorithms namely PFA, MOA, COA, and FSA.

The remaining sections of the paper are organized as follows: Section 2 describes the mathematical modelling of PV-based distributed generation systems that is suitable for load flow studies. On the third page, you will find information about voltage-dependent modelling for various types of loads and their penetration levels. In Section 4, the proposed multi-objective optimization problem for DG allocation is explained in detail with respect to the various constraints. This section covers the theoretical concept of the WSO algorithm and its simulation. Section 6 presents a number of case studies involving IEEE 33-bus and IEEE 69-bus Ethernet data networks. Section 7 of this paper concludes with a discussion of the overall conclusions reached by this paper.

2. Modelling of photovoltaic systems

Photovoltaic (PV) systems are typically incorporated into the grid via DC/AC inverters, which are more efficient. However, as seen by [24], the actual DC power generation by PV systems is reliant on meteorological and weather conditions.

$$PV_{DC(t)} = P_{PV,r} \left(\frac{G(t)}{G_{STC}} \right) - \alpha_t [T_{c(t)} - T_{c,STC}] \quad (1)$$

$$T_{c(t)} = T_{a(t)} + \left(\frac{NOCT-20}{0.8} \right) \times G(t) \quad (2)$$

$$PV_{AC(t)} = PV_{DC(t)} \times \eta_{inv} \quad (3)$$

where $PV_{DC(t)}$ and $PV_{AC(t)}$ are the DC and AC power generation by PV system, respectively; η_{inv} is the inverter efficacy, $P_{PV,r}$ is the rated PV system capacity, G_{STC} and $T_{c,STC}$ are the solar radiation and cell temperature at standard test conditions (STC), (i.e., radiation of 1 kW/m², ambient temperature of 25° C and sea level air mass (AM) of 1.5), respectively; $G(t)$ and $T_{c(t)}$ are the actual radiation and temperature on the module at a time t , respectively; α_t is the module cell temperature coefficient, NOCT is the nominal operation cell temperature value, $T_{a(t)}$ is the ambient temperature at time t .

The PV systems are mainly suitable for active power injection at a bus in the grid. However, by controlling the inverters' power factor, there is a

possibility regulated the voltage of PV system associated load bus by injecting reactive power into the grid.

$$\overline{P}_{d,i(t)} = P_{d,i(t)} - PV_{AC,i(t)} \quad (4)$$

$$\overline{Q}_{d,i(t)} = Q_{d,i(t)} - PV_{AC,i(t)} \times \tan(\varphi_{inv,i}) \quad (5)$$

where $\overline{P}_{d,i(t)}$ and $\overline{Q}_{d,i(t)}$ are the real and reactive power loads of bus- i after integrating a PV system, respectively; $P_{d,i(t)}$ and $Q_{d,i(t)}$ are the base case real and reactive power loads, respectively; $\varphi_{inv,i}$ is the inverter's operating power factor.

3. Modelling of load penetration

In general, different kinds of loads are associated with EDNs and thus, the load consumption may differ due to their dependency on voltage profile. In [25], the network performance for different kinds of loads is analysed using voltage-dependent load modelling. The active and reactive power loads of a bus can be expressed as follows:

$$\overline{P}_{d,i(t)} = P_{d,i(t)} \times \left(\frac{|V_{i(t)}|}{|V_{ref}|} \right)^{\alpha_l} \times (1 + \gamma_{p(t)}) \quad (6)$$

$$\overline{Q}_{d,i(t)} = Q_{d,i(t)} \times \left(\frac{|V_{i(t)}|}{|V_{ref}|} \right)^{\beta_l} \times (1 + \gamma_{p(t)}) \quad (7)$$

where $\overline{P}_{d,i(t)}$ and $Q_{d,i(t)}$ are the modified active and reactive power loads of bus- i , respectively; γ_{pen} is the penetration level w.r.t. base case; $|V_{i(t)}|$ and $|V_{ref}|$ are the voltage magnitude of bus- i at time- t and reference voltage, respectively; α_l and β_l are the exponents for active and reactive powers based on type of load, respectively.

4. Problem formulation

Loss minimization, voltage profile improvement, and reduction of GHG emission are aimed in this work while solving optimal allocation of PV based DGs in EDNs. A multi-objective function is defined by,

$$OF = P_{loss} + VD + GHG_{em} \quad (8)$$

$$P_{loss} = \sum_{k=1}^{nbr} (i_b^2 \times r_b) \quad (9)$$

$$VD = \frac{1}{nb} \sum_{i=1}^{nb} V_{i(t)} \quad (10)$$

$$GHG_{em} = P_{d(s/s)} \times (CO_2 + NO_x + SO_2) \quad (11)$$

where P_{loss} is the total real power losses, VD is the voltage deviation, GHG_{em} is the GHG emission, i_b and r_b are the branch current and resistance respectively; nb and nbr are the number of buses and number of branches in the network, respectively; P_D is the total load demand, CO_2 , NO_x and SO_2 are the most pollutants of conventional power plants [6].

The OF is subjected to the following equal and unequal constraints such as (i) generation-demand balance for active and reactive powers, (ii) voltage limits, (iii) branch current/MVA limits, and are given by Eqs. (12) to (15), respectively.

$$P_{d(s/s)} = P_{loss} + P_D - PV_P \quad (12)$$

$$Q_{d(s/s)} = Q_{loss} + Q_D - PV_Q \quad (13)$$

$$|V_i|_{min} \leq |V_i| \leq |V_i|_{max} \quad (14)$$

$$|I_b| \leq |I_b|_{max} \quad (15)$$

where $P_{d(s/s)}$ and $Q_{d(s/s)}$ are the active and reactive power demands of substation, respectively; P_{loss} and Q_{loss} are the active and reactive power losses, respectively; P_D and Q_D are the active and reactive power demands of the network, respectively; PV_P and PV_Q are the active and reactive power supplied by PV systems, respectively; $|V_i|_{min}$ and $|V_i|_{max}$ are the voltage magnitude minimum and maximum limits, respectively; $|I_b|$ and $|I_b|_{max}$ are the branch current and its maximum limit, respectively;

5. White shark optimizer

The great white shark may detect prey (food source) in the deep ocean. However, the food source's location within a search space is unknown. In this scenario, white sharks must look for food in the ocean's depths. White shark optimizer (WSO) used three great white shark behaviours to seek prey (i.e. the best food source) [23]: (1) movement towards prey dependent on prey movement causing wave pauses, (2) the white shark's random quest for prey at the ocean's depths, using its connected senses of hearing and smell, (3) the white shark's behaviour while searching nearby prey. In this scenario, the great white shark approaches the best white shark closest to the optimal meal. Based on these behaviours, all white shark locations will be updated to represent the best possibilities if the prey is not identified quickly.

5.1 Initialization phase:

White Shark Optimizer (WSO) is a population-based algorithm and uses uniformly distributed random number theory to generate initial population within the search space limits and is given by,

$$ws_i^j = lb_i + r \times ub_i \quad (16)$$

$$WS = \begin{bmatrix} WS_1^1 & WS_2^1 & \dots & \dots & WS_d^1 \\ WS_1^2 & WS_2^2 & \dots & \dots & WS_d^2 \\ \vdots & \vdots & \vdots & \ddots & \vdots \\ WS_1^n & WS_2^n & \dots & \dots & WS_d^n \end{bmatrix} \quad (17)$$

where ws_i^j is the initial position vector of the j th white shark in the i th dimension, lb_i and ub_i are the lower and upper limits of the search space in the i th dimension, respectively; r is a random number generated between 0 and 1; n and d are the number of population or white sharks and dimension of search variables, respectively.

The fitness of each candidate solution generated using Eq. (16) is evaluated for the defined objective function expressed in Eq. (8) and correspondingly determines the best candidate solution at the initial phase.

5.2 Movement speed towards prey:

As predators, white sharks spend much of their time hunting and tracking prey. They generally use their incredible senses of hearing, sight, and smell to track prey. After hearing a halt in the waves, a white shark moves in an undulating pattern, as seen in Eq. (18),

$$v_{k+1}^j = \alpha \left[v_k^j + f_1 \times (ws_{gb,k} - ws_k^j) \times r_1 + f_2 \times (ws_b^{v^j} - ws_k^j) \times r_2 \right], j = 1, 2, \dots, n \quad (18)$$

where j is the index of a white shark in a population size of n , v_{k+1}^j and v_k^j are the new velocity vector of j th white shark for the iteration $(k + 1)$, and current iteration k , respectively; $ws_{gb,k}$ is the global best position obtained up to k th iteration, ws_k^j is the current iteration position of j th white shark, $ws_b^{v^j}$ is j th best position vector known to the whole swarm, r_1 and r_2 are the random numbers, respectively; f_1 and f_2 are the forces developed for controlling the effect of $ws_{gb,k}$ and $ws_b^{v^j}$ on ws_k^j , and are defined in Eqs. (19) and (20) respectively; v^j is the j th index vector of a white shark reaching to best position and it is defined by Eq. (21), and α is constriction factor

which defines the convergence characteristics of WSO and is given in Eq. (22).

$$f_1 = f_{max} + (f_{max} - f_{min}) \times e^{-(4k/k)^2} \quad (19)$$

$$f_2 = f_{min} + (f_{max} - f_{min}) \times e^{-(4k/k)^2} \quad (20)$$

$$v^j = [n \times rand(1, n)] + 1 \quad (21)$$

$$\alpha = \frac{2}{|2 - \gamma - \sqrt{\gamma^2 - 4\gamma}|} \quad (22)$$

where $rand(1, n)$ is uniformly distributed random number vector in the range of $[0, 1]$, f_{min} and f_{max} are the minimum and maximum forces to be maintained for attaining a good motion by the white sharks, respectively. After number of rigorous simulations, the authors' of WSO are fixed $f_{min}=0.5$ and $f_{max}=1.5$, respectively; γ is used as acceleration coefficient and fixed to 4.125 based on analysis.

5.3 Movement towards optimal prey:

Great white sharks spend most of their time seeking for suitable prey. As a result, the white sharks' postures change. They frequently move near prey when they hear or smell its waves. In some cases, prey escapes because a white shark approaches or it is hungry. The prey's scent is often left where the white shark may sense it. In this case, the white shark follows a school of fish to random locations in quest of prey. In this scenario, white sharks approached prey using the position update mechanism outlined in Eq. (23).

$$ws_{k+1}^j = \begin{cases} ws_k^j \cdot - \oplus ws_o + u \cdot a + l \cdot b; & rand < mv \\ ws_k^j + v_k^j / F; & rand \geq mv \end{cases} \quad (23)$$

where ws_{k+1}^j is the new location vector of the j th white shark in the $(k + 1)$ th iteration step, $-$ is a negation operator, a and b are one-dimensional binary vectors defined by Eqs. (24) and (25), respectively; lb and ub are the lower and upper limits of the search space, respectively, ws_o is a logical vector defined by Eq. (26), F is the frequency of a white shark's wavy motion defined by Eqs. (27) and (28), respectively.

$$a = sgn(ws_k^j - ub) > 0 \quad (24)$$

$$b = sgn(ws_k^j - lb) > 0 \quad (25)$$

$$ws_o = \oplus (a, b) \quad (26)$$

$$F = F_{min} + \frac{F_{max} - F_{min}}{F_{max} + F_{min}} \quad (27)$$

$$mv = \frac{1}{(a_0 + e^{(k/2 - k)/a_1})} \quad (28)$$

5.4 Movement towards the best white shark:

Great white sharks can keep their position in front of the best one that is near to the prey. Eq. (29) shows how this phenomenon is expressed.

$$\overline{ws}_{k+1}^j = ws_{gb,k} + r_1 \overline{D_{p,ws}} sgn(r_2 - 0.5), \quad r_3 < S_{st} \quad (29)$$

$$\overline{D_{p,ws}} = r_3 (ws_{gb,k} - ws_k^j) \quad (30)$$

$$S_{st} = |1 - e^{(-a_2 \times k / k_{max})}| \quad (31)$$

where \overline{ws}_{k+1}^j is the current position of the j th white shark in relation to its prey, $sgn(r_2 - 0.5)$ returns either 1 or -1 to change the search direction, $\overline{D_{p,ws}}$ is the space between the white shark and the prey (i.e., food supply), S_{st} is a measure that is recommended to indicate the power of their senses of smell and sight, when white sharks following similar white sharks which are close to ideal prey, it is a measure that is recommended to indicate the power of their senses of smell and sight, a_2 is a constant value that's used to regulate actions like exploration and exploitation, k_{max} is the maximum number of iterations.

5.5 Fish school behaviour:

The initial two best answers were kept in order to mathematically recreate the behaviour of the school of white sharks, and the positions of other white sharks were updated in accordance with these best solutions. To define the fish school behaviour of white sharks, the following formula was proposed:

$$ws_{k+1}^j = \frac{ws_k^j + \overline{ws}_{k+1}^j}{2 \times r_4} \quad (32)$$

where r_1 , r_2 , r_3 , and r_4 are uniformly distributed random numbers in the range $[0, 1]$, respectively.

Eq. (32) reveals that white sharks can adjust their position in accordance with the best white shark's location, which is quite close to prey. Great white sharks' final position (as search agents) would be someplace in the search space that is extremely

close to ideal prey. The collective behaviour of WSO is identified by fish school behaviour and the movement of white sharks towards the best white shark, which expands the possibility for improved exploration and exploitation features.

6. Results and discussion

The simulations are carried out on a PC with specifications of 4 GB of RAM, a 64-bit operating system, and an Intel® Core™ i5-2410M CPU running at 2.30 GHz, with the MATLAB program.

Simulations are carried out on IEEE 33-bus standard EDN [26]. The case studies on each EDN are categorized as follows: Case 1: constant power, Case 2: residential, Case 3: commercial, and Case 4: industrial load models. Each case is repeated for three load penetration levels of 0% (base case), 25% and 50%, respectively.

6.1 Case 1: constant power load model

For the constant power (CP) load model, both α_l and β_l are equal to 0 in Eqs. (6) and (7). For base case (i.e., $\gamma_p = 0$), the load flow results are as follows: The total demand is 3715 kW and 2300 kVAr, respectively. By performing load flow [27], the network has total losses of 202.6711 kW, and 135.1409 kVAr, respectively. The minimum voltage magnitude is registered at bus-18 as 0.9131 p.u. and the average voltage deviation is observed as 0.9485 p.u. Since there are no DGs in the network, the total load and losses are supplied by main-grid. The supply from main-grid is considered as conventional fuel based sources and thus, total GHG emission is estimated at 8022.1×10^3 lb/h [6].

By optimizing the proposed objective function expressed in Eq. (8) using WSO, the best locations and sizes of PV-DGs are determined as 754.53 kW, 1071.23 kW and 1100 kW at buses 14, 24 and 30, respectively. In comparison to base case, the network performance is improved significantly. The losses are reduced to 71.4572 kW, and 49.3916 kVAr, respectively. The minimum voltage magnitude is registered at bus-33 as 0.9687 p.u. and the average voltage deviation is observed as 0.9822 p.u. Since network as PV-DGs, the total load and losses are supplied by main-grid are decreased, thus, total GHG emission is reduced to 1761.9×10^3 lb/h.

The results of WSO are compared with literature works and given in Table 1. In comparison to SSA [1], WCA [6], and GA [13], WSO results are superior in terms of global optima. On the other hand, WSO is performed highly competitive to EGWO-PSO [7], HHO-PSO [10] and Jaya [14]. In

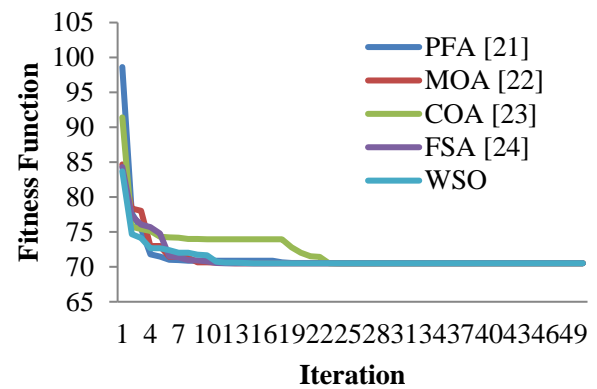


Figure. 1 Convergence characteristics of different algorithms

Table 1, (*) indicates the re-simulation of load flow with the solution given by that corresponding algorithm.

In Table 2, the computational efficiency of WSO is quantified using 50 independent simulations of PFA [28], MOA [29], COA [30] and FSA [31] and WSO. The convergence characteristics of these algorithms for best results are given in Fig. 1.

Similarly, WSO is extended to find PV allocation for different penetration levels of load. The network performances without PVs and with optimal PVs for different penetrations are given in Table 3.

It can be seen that the overall performance is improved significantly with optimal PV allocation in the network irrespective of loading levels.

6.2 Case 2: residential load model

For residential load model, the $\alpha_l = 0.92$ and $\beta_l = 4.04$ are in Eqs. (6) and (7), and the outcomes are as follows: Total demand is 3564.55 kW and 1885.06 kVAr. Load flow results in network losses of 159.336 kW and 105.851 kVAr. Bus-18 has a minimum voltage of 0.9234 p.u. and an average voltage deviation of 0.9544 p.u. Because there are no DGs in the network, main-grid supplies all load and losses. The main-grid supply is considered fossil fuel based, hence overall GHG emissions are estimated as 7625.256×10^3 lb/h.

Using WSO to optimize the proposed objective function Eq. (8), the best placements and sizes of PV-DGs are determined to be buses 24, 30, and 14. The sizes in kW are, 1065.36, 942.64, and 714.64, respectively. The network performance is much better than the base scenario. The losses are now 60.1361 kW and 41.4619 kVAr. Bus-33 has a minimum voltage of 0.9672 p.u. and an average voltage deviation of 0.9814 p.u. Since PV-DGs

Table 1. Comparison of WSO' performance with literature works

Algorithm	PV size in kW (bus #)	P _{loss} (kW)	Q _{loss} (kW)	V _{min} in p.u. (bus #)	VD (p.u.)	GHG _{em} (lb/h)×10 ³
Base	-	202.6711	135.1409	0.9131 (18)	0.9485	8022.1
SSA [1]*	753.6 (13), 1100.4 (23), 1070.6 (29)	76.0102	52.8281	0.9651 (33)	0.9810	1773.3
WCA [6]*	854.6 (14), 1101.7 (24), 1181 (29)	72.9586	50.6075	0.9697 (33)	0.9850	1330.9
EGWO-PSO [7]	754 (14), 1099 (24), 1071 (30)	71.4572	49.3900	0.9686 (33)	0.9822	1764.3
HHO-PSO [10]*	761.4 (14), 1094.7 (24), 1068 (30)	71.4595	49.3893	0.9686 (33)	0.9823	1766.0
GA [13]*	761 (14), 1170 (240), 1082 (30)	71.5355	49.5225	0.9694 (33)	0.9827	1583.9
Jaya [14]*	755.59 (14), 1097.04 (24), 1071.6 (30)	71.4572	49.3900	0.9686 (33)	0.9822	1764.3
WSO	754.53 (14), 1071.23 (30), 1100 (24)	71.4572	49.3916	0.9687 (33)	0.9822	1764.3

Table 2. Comparison of WSO' performance with other algorithms

Algorithm	PV size in kW (bus #)	P _{loss} (kW)	VD (p.u.)	GHG _{em} (lb/h)×10 ³	Parameters		
					mean	median	std.
PFA [21]	854.50 (14), 1102 (24), 1182 (29)	74.56	0.9706	1402.011	71.466	70.523	4.104
MOA [22]	755.78 (14), 1100 (24), 1083.04 (30)	71.46	0.9824	1764.298	71.268	70.517	2.495
COA [23]	1084.4 (30), 756.49 (14), 1085.62 (24)	71.46	0.9824	1764.298	72.330	70.520	3.281
FSA [24]	756.49 (14), 1084.4 (30), 1085.62 (24)	71.46	0.9824	1764.298	71.289	70.517	2.410
WSO	754.53 (14), 1071.23 (30), 1100 (24)	71.46	0.9822	1764.298	71.178	70.517	2.034

Table 3. WSO' performance for constant power (CP) load model with different penetration levels

γ _p (%)	Without PVs			With PVs			
	P _{loss} (kW)	VD (p.u.)	GHG _{em} (lb/h)×10 ³	PV size in kW (bus #)	P _{loss} (kW)	VD (p.u.)	GHG _{em} (lb/h)×10 ³
0	202.6766	0.9485	8022.07	1071.42(30), 753.98 (14), 1099.44 (24)	71.457	0.9822	1764.298
0.25	329.8519	0.9342	10184.25	1275.14(30), 966.49 (14), 1372.71 (24)	113.610	0.9770	2340.516
0.5	496.3486	0.9192	12426.94	1141.02(14), 1671.24 (24), 1632.46 (30)	166.040	0.9731	2649.304

Table 4. WSO' performance for residential load model with different penetration levels

γ _p (%)	Without PVs			With PVs			
	P _{loss} (kW)	VD (p.u.)	GHG _{em} (lb/h)×10 ³	PV size in kW (bus #)	P _{loss} (kW)	VD (p.u.)	GHG _{em} (lb/h)×10 ³
0	159.336	0.9544	7625.256	1065.36(24), 942.64 (30), 714.64 (14)	60.136	0.9814	2125.866
0.25	244.008	0.9436	9532.101	1155.78(30), 1328.80 (24), 886.66 (14)	91.365	0.9766	2745.024
0.5	344.986	0.9331	11437.75	1056.82 (14), 1591.03 (24), 1363.05 (30)	127.967	0.9718	3388.422

Table 5. WSO' performance for commercial load model with different penetration levels

γ _p (%)	Without PVs			With PVs			
	P _{loss} (kW)	VD (p.u.)	GHG _{em} (lb/h)×10 ³	PV size in kW (bus #)	P _{loss} (kW)	VD (p.u.)	GHG _{em} (lb/h)×10 ³
0	154.935	0.9551	7433.643	717.10 (14), 954.97 (30), 1066.42 (24)	61.456	0.9815	2079.159
0.25	235.125	0.9447	9237.393	1330.28(24), 889.79 (14), 1172.00 (30)	93.821	0.9766	2679.978
0.5	329.207	0.9346	11019.5	1060.35 (14), 1382.56 (30), 1592.90 (24)	132.004	0.9718	3304.880

Table 6. WSO' performance for industrial load model with different penetration levels

γ _p (%)	Without PVs			With PVs			
	P _{loss} (kW)	VD (p.u.)	GHG _{em} (lb/h)×10 ³	PV size in kW (bus #)	P _{loss} (kW)	VD (p.u.)	GHG _{em} (lb/h)×10 ³
0	161.698	0.9543	7876.426	706.13 (14), 909.91 (30), 1058.30 (24)	56.098	0.9814	2239.563
0.25	250.867	0.9432	9926.201	1318.69 (24), 875.97 (14), 1114.44 (30)	84.001	0.9768	2894.779
0.5	360.334	0.9323	12009.72	1577.77 (24), 1315.51 (30), 1044.70 (14)	116.114	0.9722	3569.647

reduce main-grid load and losses, overall GHG emissions are lowered to 2125.866×10^3 lb/h.

In a similar vein, WSO has been extended to find PV allocation for different levels of load penetration. According to the penetration levels shown in Table 4, the network's performances without PVs and with optimal PVs are both excellent.

6.3 Case 3: commercial load model

In Eqs. (6) and (7), the $\alpha_l = 1.51$ and $\beta_l = 3.4$ are to be considered for this load model. The load flow results for the base scenario are: 3475.38 kW and 1948.15 kVAr total demand. There are 154.935 kW and 102.872 kVAr losses when executing load flow. Bus-18 has a minimum voltage of 0.9246 p.u. and an average voltage deviation of 0.9551 p.u.. It is fed by main-grid because there are no DGs. So the overall GHG emissions are calculated as 7433.64×10^3 lb/h from main-grid supply.

Using WSO to optimize the proposed objective function Eq. (8), the best placements and sizes of PV-DGs are determined to be buses 14, 30, and 24. The sizes in kW are: 717.10, 954.97, and 1066.42, respectively. The network performance is much better than the base scenario. These locations and sizes are found by maximizing the proposed objective function. The network performance is much better than in the base situation. The losses are 61.456 kW and 42.333 kVAr. Bus-33 measures 0.9673 p.u. minimum voltage and 0.9815 p.u. average voltage deviation. A reduction in main-grid load and losses reduces GHG emissions to 2079.16×10^3 lb/h.

6.4 Case 4: industrial load model

In Eqs. (6) and (7), the $\alpha_l = 0.18$ and $\beta_l = 6$ are to be considered for this load model. The results for the base case are as follows: Total demand is 3684.85 kW and 1717.78 kVAr. Load flow results in losses of 161.698 kW and 107.486 kVAr. Bus-18 has a minimum voltage magnitude of 0.9228 p.u. and an average voltage deviation of 0.9543 p.u. Since there are no DGs in the network, main-grid supplies all load and losses. The main-grid supply is deemed fossil fuel based, hence total GHG emission is estimated as 7876.426×10^3 lb/h.

Using WSO to optimize the proposed objective function, the best placements and sizes of PV-DGs are identified to be buses 14, 30, and 24. The optimal sizes in kW are: 706.13, 909.91, 1058.30, respectively. The network performance is much better than base case. The losses drop to 56.097 kW

and 38.733 kVAr. Bus-33 has a minimum voltage magnitude of 0.9673 p.u. and an average voltage deviation of 0.9814 p.u. Since PV-DGs reduce main-grid load and losses, overall GHG emission is lowered to 2239.563×10^3 lb/h.

Similarly, simulations are repeated for an increased penetration level of 25% and 50% and the best results obtained by WSO are given in Table 5 and Table 6, for the commercial and industrial load models, respectively. From these results, it can be said that the optimal allocation of PV-based DGs in EDN can result for improved operation irrespective of increased load penetration levels.

7. Conclusion

The optimal allocation of PV-based DG allocation problem in EDN is solved using a new and efficient nature-inspired meta-heuristic method white shark optimizer (WSO). Loss minimization, voltage profile improvement, and GHG reduction are among the multi-objective problems tackled. In addition, the simulations in IEEE 33-bus EDN are extended to include several types of loads, including as residential, industrial, and commercial, as well as their various penetration levels. In addition, the proposed methodology is resulted for loss reduction by 64.74%, 62.26%, 60.33%, and 65.31% for constant power, residential, commercial and industrial load models at base case. On the other side, the GHG emission is reduced 78%, 72.12%, 72.03%, and 71.57% for constant power, residential, commercial and industrial load models at base case. The results of a comparison of PFA, MOA, COA FSA, and WSO are presented. In terms of global optima and computing time, WSO's results have been found to be superior. Furthermore, regardless of higher load penetration levels, the proper deployment of PV-based DGs in EDN can result in overall improved operation. However, the emerging electric vehicles (EVs) and their stochastic nature needs to be considered while solving the intermittency nature RE-based DGs, so that a cooperative and effective operation can be achieved in modern EDNs.

Conflicts of Interest

Authors declare that no conflicts of interest.

Author Contributions

The supervision, review of work and project administration, has been done by Anitha M. The paper background work, conceptualization, and methodology have been done by Kotaiah N.C. The

dataset collection and editing draft is prepared by Rajesh Patil. The program implementation, result analysis and comparison, and visualization have been done by Nagaraja Kumari.CH.

References

- [1] K. S. Sambaiah and T. Jayabarathi, "Optimal allocation of renewable distributed generation and capacitor banks in distribution systems using salp swarm algorithm", *International Journal of Renewable Energy Research*, Vol. 9, No. 1, pp. 96-107, 2019.
- [2] A. M. Shaheen and R. A. E. Sehiemy, "Optimal coordinated allocation of distributed generation units/capacitor banks/voltage regulators by EGWA", *IEEE Systems Journal*, Vol. 15, No. 1, pp. 257-264, 2021.
- [3] A. M. Eltamaly, Y. S. Mohamed, A. H. E. Sayed, M. A. Mohamed, and A. N. Elghaffar, "Power quality and reliability considerations of photovoltaic distributed generation", *Technology and Economics of Smart Grids and Sustainable Energy*, Vol. 5, No. 25, pp. 1-21, 2020.
- [4] K. Mahmoud and M. Lehtonen, "Simultaneous allocation of multi-type distributed generations and capacitors using generic analytical expressions", *IEEE Access*, Vol. 7, pp. 182701-182710, 2019.
- [5] S. R. Gampa, K. Jasthi, P. Goli, D. Das, and R. C. Bansal, "Grasshopper optimization algorithm based two stage fuzzy multiobjective approach for optimum sizing and placement of distributed generations, shunt capacitors and electric vehicle charging stations", *Journal of Energy Storage*, Vol. 27, 101117, 2020.
- [6] A. A. Abou, E. Ela, R. A. E. Sehiemy, and A. S. Abbas, "Optimal placement and sizing of distributed generation and capacitor banks in distribution systems using water cycle algorithm", *IEEE Systems Journal*, Vol. 12, No. 4, pp. 3629-3636, 2018.
- [7] C. Venkatesan, R. Kannadasan, M. H. Alsharif, M. K. Kim, and J. Nebhen, "A novel multiobjective hybrid technique for siting and sizing of distributed generation and capacitor banks in radial distribution systems", *Sustainability*, Vol. 13, No. 6, 3308, 2021.
- [8] P. D. Huy, V. K. Ramachandaramurthy, J. Y. Yong, K. M. Tan, and J. B. Ekanayake, "Optimal placement, sizing and power factor of distributed generation: A comprehensive study spanning from the planning stage to the operation stage", *Energy*, Vol. 195, 117011, 2020.
- [9] V. Janamala and K. R. Rani, "Optimal allocation of solar photovoltaic distributed generation in electrical distribution networks using Archimedes optimization algorithm", *Clean Energy*, Vol. 6, No. 2, pp. 1036-1052, 2022.
- [10] M. R. Elkadeem, M. A. Elaziz, Z. Ullah, S. Wang, and S. W. Sharshir, "Optimal planning of renewable energy-integrated distribution system considering uncertainties", *IEEE Access*, Vol. 7, 164887-164907, 2019.
- [11] A. Selim, S. Kamel, A. S. Alghamdi, and F. Jurado, "Optimal placement of DGs in distribution system using an improved harris hawks optimizer based on single-and multi-objective approaches", *IEEE Access*, Vol. 8, pp. 52815-52829, 2020.
- [12] E. A. Almabsout, R. A. E. Sehiemy, O. An, and O. Bayat, "A hybrid local search-genetic algorithm for simultaneous placement of DG units and shunt capacitors in radial distribution systems", *IEEE Access*, Vol. 8, pp. 54465-54481, 2020.
- [13] T. K. Pandraju and V. Janamala, "Butterfly Optimization Algorithm-Based Optimal Sizing and Integration of Photovoltaic System in Multi-lateral Distribution Network for Interoperability", *Lecture Notes in Networks and Systems*, Vol. 204, pp. 201-209, 2021.
- [14] M. D. Hraiz, J. A. García, R. J. Castañeda, and H. Muhsen, "Optimal PV size and location to reduce active power losses while achieving very high penetration level with improvement in voltage profile using modified Jaya algorithm", *IEEE Journal of Photovoltaics*, Vol. 10, No. 4, pp. 1166-1174, 2020.
- [15] U. Raut and S. Mishra, "A new Pareto multi-objective sine cosine algorithm for performance enhancement of radial distribution network by optimal allocation of distributed generators", *Evolutionary Intelligence*, Vol. 14, No. 4, pp. 1635-1656, 2021.
- [16] F. A. Zeidabadi, S. A. Doumari, M. Dehghani, and O. P. Malik, "MLBO: Mixed leader based optimizer for solving optimization problems", *International Journal of Intelligent Engineering and Systems*, Vol. 14, No. 4, pp. 472-479, 2021, doi: 10.22266/ijies2021.0831.41.
- [17] F. A. Zeidabadi, M. Dehghani, and O. P. Malik, "TIMBO: Three influential members based optimizer", *International Journal of Intelligent Engineering and Systems*, Vol. 14, No. 5, pp.

- 121-128, 2021, doi: 10.22266/ijies2021.1031.12.
- [18] M. Dehghani, Z. Montazeri, H. Givi, J. M. Guerrero, and G. Dhiman, "Darts game optimizer: a new optimization technique based on darts game", *International Journal of Intelligent Engineering and Systems*, Vol. 13, No. 5, pp. 286-294, 2020, doi: 10.22266/ijies2020.1031.26.
- [19] S. A. Doumari, F. A. Zeidabadi, M. Dehghani, and O. P. Malik, "Mixed best members based optimizer for solving various optimization problems", *International Journal of Intelligent Engineering and Systems*, Vol. 14, No. 4, pp. 384-392, 2021, doi: 10.22266/ijies2021.0831.34.
- [20] M. Dehghani, Z. Montazeri, A. Dehghani, R. A. R. Mendoza, H. Samet, J. M. Guerrero, and G. Dhiman, "MLO: Multi leader optimizer", *International Journal of Intelligent Engineering and Systems*, Vol. 13, No. 6, pp. 364-373, 2020, doi: 10.22266/ijies2020.1231.32.
- [21] F. A. Zeidabadi, M. Dehghani, and O. P. Malik, "RSLBO: Random selected leader based optimizer", *International Journal of Intelligent Engineering and Systems*, Vol. 14, No. 5, pp. 529-538, 2021, doi: 10.22266/ijies2021.1031.46.
- [22] Q. T. Nguyen and M. P. Bui, "Performance of equilibrium optimizer for the traveling salesman problem", *International Journal of Intelligent Engineering and Systems*, Vol. 14, No. 5, pp. 46-55, 2021, doi: 10.22266/ijies2021.1031.05.
- [23] M. Braik, A. Hammouri, J. Atwan, M. A. A. Betar, and M. A. Awadallah, "White Shark Optimizer: A novel bio-inspired meta-heuristic algorithm for global optimization problems", *Knowledge-Based Systems*, Vol. 243, 108457, 2022.
- [24] R. Dabou, F. Bouchafaa, A. H. Arab, A. Bouraiou, M. D. Draou, A. Neçaibia, and M. Mostefaoui, "Monitoring and performance analysis of grid connected photovoltaic under different climatic conditions in south Algeria", *Energy Conversion and Management*, Vol. 130, pp. 200-206, 2016.
- [25] V. Janamala and T. K. Pandraju, "Static voltage stability of reconfigurable radial distribution system considering voltage dependent load models", *Mathematical Modelling of Engineering Problems*, Vol. 7, No. 3, pp. 450-458, 2020.
- [26] M. E. Baran and F. F. Wu, "Network reconfiguration in distribution systems for loss reduction and load balancing.", *IEEE Transactions on Power Delivery*, 4(2), 1401-1407, 1989.
- [27] R. D. Zimmerman, C. E. M. Sánchez, and R. J. Thomas, "MATPOWER: Steady-state operations, planning, and analysis tools for power systems research and education", *IEEE Transactions on Power Systems*, Vol. 26, No. 1, pp. 12-19, 2010.
- [28] H. Yapici and N. Cetinkaya, "A new meta-heuristic optimizer: Pathfinder algorithm", *Applied Soft Computing*, Vol. 78, pp. 545-568, 2019.
- [29] K. Zervoudakis and S. Tsafarakis, "A mayfly optimization algorithm", *Computers & Industrial Engineering*, Vol. 145, 106559, 2020.
- [30] J. Pierezan and L. D. Coelho, "Coyote optimization algorithm: a new metaheuristic for global optimization problems", In: *Proc. of 2018 IEEE Congress on Evolutionary Computation*, pp. 1-8, 2018.
- [31] M. Elsis, "Future search algorithm for optimization", *Evolutionary Intelligence*, Vol. 12, pp. 21-31, 2019.